

Vacuum fluctuation effects on hyperonic neutron star matter^{*}

WENG Ming-Hua(翁铭华)^{1,2;1)} GUO Xin-Heng(郭新恒)^{2;2)} LIU Bo(刘波)^{3;3)}

¹ Department of Physics and Electronic Information Engineering, Minjiang University, Fuzhou 350108, China

² College of Nuclear Science and Technology, Beijing Normal University, Beijing 100875, China

³ Institute of High Energy Physics, Chinese Academy of Sciences, Beijing 100049, China

Abstract: The vacuum fluctuation (VF) effects on the properties of the hyperonic neutron star matter are investigated in the framework of the relativistic mean field (RMF) theory. The VF corrections result in the density dependence of in-medium baryon and meson masses. We compare our results obtained by adopting three kinds of meson-hyperon couplings. The introduction of both hyperons and VF corrections softens the equation of state (EoS) for the hyperonic neutron star matter and hence reduces hyperonic neutron star masses. The presence of the δ field enlarges the masses and radii of hyperonic neutron stars. Taking into account the uncertainty of meson-hyperon couplings, the obtained maximum masses of hyperonic neutron stars are in the range of $1.33M_{\odot}$ – $1.55M_{\odot}$.

Key words: equations of state of the neutron star matter, hyperons

PACS: 26.60.Kp, 14.20.Jn **DOI:** 10.1088/1674-1137/37/12/125101

1 Introduction

The nonlinear Walecka model (NLWM), based on the relativistic mean field (RMF) theory, has been successfully used in the study of nuclear matter and neutron stars [1–7]. Neutron stars are composed of highly compressed matter. Nuclear matter at high densities exhibits a new degree of freedom: strangeness. Hyperons, kaon condensation, and quarks may appear in neutron stars, and these complicated compositions of neutron stars have attracted much attention. The important property of a neutron star is characterized by its mass and radius, which can be obtained from the appropriate equation of state (EoS) at high densities. The RMF model was first used to investigate the properties of hyperonic neutron stars (npe μ H) (H denotes hyperons throughout this paper) in the 1980s [8, 9]. Recently, in some studies based on the RMF model, it has been indicated that the strangeness is a new degree of freedom in neutron star matter [10–12]. In recent years it has been stressed that the inclusion of the δ field is important in the study of the asymmetric nuclear matter [6, 7, 12–14]. The inclusion of the δ field leads to the structure of relativistic interactions, where a balance between an attractive (scalar) and a repulsive (vector) potential exists.

The δ field plays a role in the isospin channel and mainly affects the behavior of the system in the high density regions and so is of great interest in nuclear astrophysics. The influence of the δ field on the properties of hyperonic neutron stars has been investigated based on the RMF model [12, 15, 16].

In Ref. [17], the vacuum fluctuation (VF) corrections were taken into account to study the properties of nuclear matter. Recently, the VF-RMF model was developed by including the isovector mesons (ρ and δ) to investigate the properties of the asymmetric nuclear matter and neutron stars [18]. The VF effects lead to the dependence of in-medium hadron masses on the total baryon density. In this work, we will extend the VF-RMF model to hyperon-rich matter in neutron stars by including the hyperons and leptons in the relativistic Lagrangian density. The VF effects will be introduced by considering loop corrections in the self-energies of in-medium baryons and mesons as in Ref. [18]. The VF effects on the properties of the hyperonic neutron star matter will be studied.

This article is organized as follows. In Section 2, we derive the in-medium masses of baryons and mesons and the EoS for the hyperonic neutron star matter in the VF-RMF model. Section 3 is devoted to our results and discussions. In Section 4, a brief summary is presented.

Received 27 February 2013, Revised 16 July 2013

^{*} Supported by National Natural Science Foundation of China (10975018, 11175020, 11275025, 11075037, and 11247287), Fundamental Research Funds for Central Universities in China and Natural Science Foundation of Fujian Province (2012J05122)

1) E-mail: mhweng@mju.edu.cn; mhweng@mail.bnu.edu.cn

2) E-mail: xhguo@bnu.edu.cn (corresponding author)

3) E-mail: liub@mail.ihep.ac.cn (corresponding author)

©2013 Chinese Physical Society and the Institute of High Energy Physics of the Chinese Academy of Sciences and the Institute of Modern Physics of the Chinese Academy of Sciences and IOP Publishing Ltd

2 The baryon octet VF-RMF model

The relativistic Lagrangian density with the baryon octet and free leptons used in this work reads

$$\begin{aligned} \mathcal{L} = & \sum_B \bar{\psi}_B [i\gamma_\mu \partial^\mu - (M_B - g_{\sigma B} \phi - g_{\delta B} \vec{t}_B \cdot \vec{\delta}) - g_{\omega B} \gamma_\mu \omega^\mu \\ & - g_{\rho B} \gamma^\mu \vec{t}_B \cdot \vec{b}_\mu] \psi_B + \frac{1}{2} (\partial_\mu \phi \partial^\mu \phi - m_\sigma^2 \phi^2) - U(\phi) \\ & + \frac{1}{2} m_\omega^2 \omega_\mu \omega^\mu + \frac{1}{2} m_\delta^2 \vec{b}_\mu \cdot \vec{b}^\mu + \frac{1}{2} (\partial_\mu \vec{\delta} \cdot \partial^\mu \vec{\delta} - m_\delta^2 \vec{\delta}^2) \\ & - \frac{1}{4} F_{\mu\nu} F^{\mu\nu} - \frac{1}{4} \vec{G}_{\mu\nu} \vec{G}^{\mu\nu} + \sum_l \bar{\psi}_l (i\gamma_\mu \partial^\mu - m_l) \psi_l + \delta\mathcal{L}, \end{aligned} \quad (1)$$

where the sum on B is over all the states of the lowest baryon octet (with mass M_B) ($B=n, p, \Lambda, \Sigma^-, \Sigma^0, \Sigma^+, \Xi^-, \Xi^0$) and the sum on l is over the free leptons (with mass m_l) ($l=e^-, \mu^-$); $\phi, \omega_\mu, \vec{b}_\mu$, and $\vec{\delta}$ (with masses $m_\sigma, m_\omega, m_\rho, m_\delta$, respectively) represent σ, ω, ρ , and δ meson fields, respectively; \vec{t}_B represents the isospin generator matrix for the baryon B; $U(\phi) = \frac{1}{3}a\phi^3 + \frac{1}{4}b\phi^4$ is the nonlinear potential of the σ meson, $F_{\mu\nu} \equiv \partial_\mu \omega_\nu - \partial_\nu \omega_\mu$ and $\vec{G}_{\mu\nu} \equiv \partial_\mu \vec{b}_\nu - \partial_\nu \vec{b}_\mu$; the counterterm for the Lagrangian density, $\delta\mathcal{L}$, has the same form as that in Ref. [18].

The field equation for the baryon B in the RMF approximation is given by

$$\begin{aligned} [i\gamma_\mu \partial^\mu - (M_B - g_{\sigma B} \phi - g_{\delta B} t_{3B} \delta_3) \\ - g_{\omega B} \gamma^0 \omega_0 - g_{\rho B} \gamma^0 t_{3B} b_0] \psi_B = 0, \end{aligned} \quad (2)$$

with

$$\begin{aligned} \phi &= \frac{1}{m_\sigma^2} \left(\sum_B g_{\sigma B} \rho_{sB} - a\phi^2 - b\phi^3 \right), \\ \omega_0 &= \frac{1}{m_\omega^2} \sum_B g_{\omega B} \rho_B, \\ b_0 &= \frac{1}{m_\rho^2} \sum_B g_{\rho B} t_{3B} \rho_B, \\ \delta_3 &= \frac{1}{m_\delta^2} \sum_B g_{\delta B} t_{3B} \rho_B^s, \end{aligned} \quad (3)$$

where t_{3B} is the third direction projection of the \vec{t}_B for the baryon B. ρ_B and ρ_B^s are the number and scalar densities of the baryon B, which are given in the following respectively,

$$\rho_B = \frac{k_{FB}^3}{3\pi^2}, \quad (4)$$

and

$$\rho_B^s = -i \int \frac{d^4 k}{(2\pi)^4} \text{Tr} G^B(k), \quad (5)$$

where k_{FB} is the Fermi momentum of the baryon B and $G^B(k)$ is the propagator of the baryon B in the VF-RMF model:

$$\begin{aligned} G^B(k) &= (\gamma_\mu k^\mu + M_B^*) \left[\frac{1}{k^2 - M_B^{*2} + i\eta} \right. \\ &\quad \left. + \frac{i\pi}{E_{FB}^*} \delta(k^0 - E_{FB}) \theta(k_{FB} - |\vec{k}|) \right] \\ &\equiv G_F^B(k) + G_D^B(k), \end{aligned} \quad (6)$$

where M_B^* is the effective mass of the baryon B, $E_{FB}^{(*)} = \sqrt{k_{FB}^2 + M_B^{(*)2}$ and η is infinitesimal.

In the present work, we only consider the dominant VF contributions from the tadpole diagrams to the self-energies of baryon octet states. Thus, when the VF corrections are introduced through Fig. 1(a), the effective mass of the baryon B can be written as:

$$\begin{aligned} M_B^* &= M_B + ig_{\sigma B} \sum_{B'} \frac{g_{\sigma B'}}{m_\sigma^{*2}} \int \frac{d^4 k}{(2\pi)^4} \text{Tr} G^{B'}(k) \\ &\quad + ig_{\delta B} t_{3B} \sum_{B'} \frac{g_{\delta B'}}{m_\delta^{*2}} t_{3B'} \int \frac{d^4 k}{(2\pi)^4} \text{Tr} G^{B'}(k) \\ &\quad + \frac{g_{\sigma B}}{m_\sigma^{*2}} (a\phi^2 + b\phi^3), \end{aligned} \quad (7)$$

where m_j^* ($j=\sigma, \omega, \rho, \delta$ throughout this paper) are the off-shell in-medium meson masses.

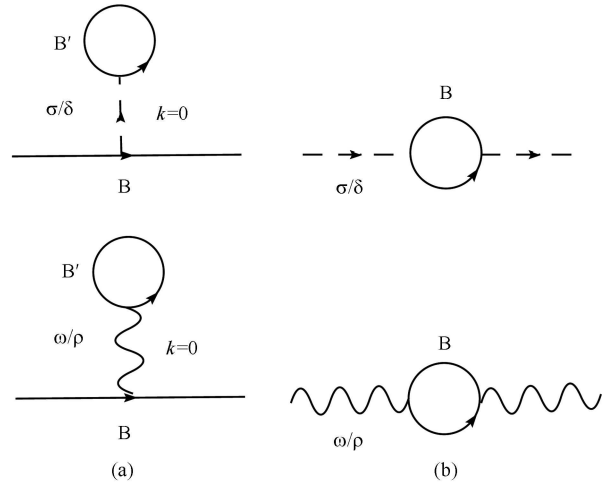


Fig. 1. Loop-diagram corrections to the self-energy of baryon octet states (a) and mesons (b) in medium, where B' denotes baryons and k is the four momentum of the meson.

The introduction of the density dependence of the in-medium meson masses is the critical effect of VF corrections. Because the meson propagators in the baryon

self-energies carry zero four-momenta, we must use the off-shell ($q^\mu = 0$) meson masses in the tadpole loop calculations for self consistency. We calculate the in-medium meson masses in the random-phase approximation (RPA) [17, 19], see Fig. 1(b). The obtained off-shell effective mass of the σ meson is given by

$$m_\sigma^{*2} = m_\sigma^2 + \Pi_\sigma(q^\mu = 0), \quad (8)$$

where

$$\Pi_\sigma(q^\mu = 0) = -i \sum_B g_{\sigma B}^2 \int \frac{d^4 k}{(2\pi)^4} \text{Tr}[G^B(k+q)G^B(k)]. \quad (9)$$

The off-shell effective mass of the δ meson is obtained as follows:

$$m_\delta^{*2} = m_\delta^2 + \Pi_\delta(q^\mu = 0), \quad (10)$$

where

$$\Pi_\delta(q^\mu = 0) = -i \sum_B g_{\delta B}^2 t_{3B}^2 \int \frac{d^4 k}{(2\pi)^4} \text{Tr}[G^B(k+q)G^B(k)]. \quad (11)$$

The off-shell effective mass of the ω meson is given by

$$m_\omega^{*2} = m_\omega^2 + \Pi_{\omega T}(q^\mu = 0), \quad (12)$$

where $\Pi_{\omega T}$ is the transverse part of the following polarization tensor:

$$\Pi_{\omega}^{\mu\nu}(q^\mu = 0) = -i \sum_B g_{\omega B}^2 \int \frac{d^4 k}{(2\pi)^4} \text{Tr}[\gamma^\mu G^B(k+q)\gamma^\nu G^B(k)]. \quad (13)$$

The off-shell effective mass of the ρ meson is given by

$$m_\rho^{*2} = m_\rho^2 + \Pi_{\rho T}(q^\mu = 0), \quad (14)$$

where $\Pi_{\rho T}$ is the transverse part of the following polarization tensor:

$$\begin{aligned} \Pi_{\rho}^{\mu\nu}(q^\mu = 0) &= -i \sum_B g_{\rho B}^2 t_{3B}^2 \int \frac{d^4 k}{(2\pi)^4} \\ &\times \text{Tr}[\gamma^\mu G^B(k+q)\gamma^\nu G^B(k)]. \end{aligned} \quad (15)$$

Obviously, the modification of the in-medium hadron masses will affect the properties of the hyperonic neutron star matter. The meson masses appearing in the Lagrangian density should be replaced by the off-shell in-medium meson masses in our calculations. Therefore, the energy-momentum tensor in the VF-RMF model can be expressed as

$$\begin{aligned} T_{\mu\nu} &= \sum_B i\bar{\psi}_B \gamma_\mu \partial_\nu \psi_B + \sum_1 i\bar{\psi}_1 \gamma_\mu \partial_\nu \psi_1 + g_{\mu\nu} \left[\frac{1}{2} m_\sigma^{*2} \phi^2 \right. \\ &\left. + U(\phi) - \frac{1}{2} m_\omega^{*2} \omega_\lambda \omega^\lambda - \frac{1}{2} m_\rho^{*2} b_\lambda^\vec{r} b^{\vec{\lambda}} + \frac{1}{2} m_\delta^{*2} \delta^{\vec{2}} \right]. \end{aligned} \quad (16)$$

The EoS for the hyperonic neutron star matter is given by the diagonal components of the energy-momentum tensor. Thus we have the energy density as follows:

$$\begin{aligned} \epsilon &= -i \sum_B \int \frac{d^4 k}{(2\pi)^4} \text{Tr}[\gamma^0 G^B(k)] k^0 \\ &+ \sum_1 \frac{1}{8\pi^2} \left[k_{F_1} E_{F_1}^* (m_1^2 + 2k_{F_1}^2) - m_1^4 \ln \left(\frac{k_{F_1} + E_{F_1}^*}{m_1} \right) \right] \\ &+ \frac{1}{2} m_\sigma^{*2} \phi^2 + U(\phi) + \frac{1}{2} m_\omega^{*2} \omega_0^2 + \frac{1}{2} m_\rho^{*2} b_0^2 + \frac{1}{2} m_\delta^{*2} \delta_3^2, \end{aligned} \quad (17)$$

and the pressure is given by

$$\begin{aligned} P &= -\frac{i}{3} \sum_{B,i} \int \frac{d^4 k}{(2\pi)^4} \text{Tr}[\gamma^i G^B(k)] k^i \\ &+ \sum_1 \frac{1}{8\pi^2} \left[m_1^4 \ln \left(\frac{k_{F_1} + E_{F_1}^*}{m_1} \right) - E_{F_1}^* k_{F_1} \left(m_1^2 - \frac{2}{3} k_{F_1}^2 \right) \right] \\ &- \frac{1}{2} m_\sigma^{*2} \phi^2 - U(\phi) + \frac{1}{2} m_\omega^{*2} \omega_0^2 + \frac{1}{2} m_\rho^{*2} b_0^2 - \frac{1}{2} m_\delta^{*2} \delta_3^2, \end{aligned} \quad (18)$$

where the sum on i is over the space components of γ and k , k_{F_1} is the Fermion momentum of free leptons and $E_{F_1} = \sqrt{m_1^2 + k_{F_1}^2}$.

Hyperonic neutron stars are neutral charged objects in β equilibrium. For the hyperonic neutron star matter, the chemical potential of baryon octet states and leptons are constrained by the baryon number and electric charge conservation:

$$\mu_\mu = \mu_e, \quad (19)$$

$$\mu_p = \mu_n - \mu_e, \quad (20)$$

$$\mu_\Lambda = \mu_{\Sigma^0} = \mu_{\Xi^0} = \mu_n, \quad (21)$$

$$\mu_{\Sigma^-} = \mu_{\Xi^-} = \mu_n + \mu_e, \quad (22)$$

$$\mu_{\Sigma^+} = \mu_p = \mu_n - \mu_e, \quad (23)$$

where μ_n and μ_e are the independent neutron and electron chemical potentials, respectively, where the chemical potentials of the baryon B and the lepton l are given by, respectively,

$$\mu_B = \sqrt{k_B^2 + M_B^{*2}} + g_{\omega B} \omega_0 + g_{\rho B} t_{3B} b_0, \quad (24)$$

$$\mu_l = \sqrt{k_{F_1}^2 + m_l^2}. \quad (25)$$

The neutral charged condition of the hyperonic neutron star matter can be expressed as:

$$\rho_p + \rho_{\Sigma^+} - \rho_{\Sigma^-} - \rho_{\Xi^-} = \rho_e - \rho_{\mu^-}. \quad (26)$$

The properties of hyperonic neutron stars can be obtained by solving Tolmann-Oppenheimer-Volkov (TOV) equations [20] with the derived EoS as the input.

3 Results and discussions

In this work, the meson-nucleon coupling constants are fixed by the same saturation properties of the nuclear matter as in Ref. [18]. In general, the interactions between different meson and hyperon states should be different. We prefer to adopt the hyperon potentials to determine the σ meson-hyperon coupling constants with the vector and isovector meson-hyperon couplings fixed by $SU(6)$ quark symmetry. For the meson-hyperon coupling constants, it is convenient to define $x_{jH} = g_{jH}/g_{jN}$ ($N=n, p$ throughout this paper). The σ meson-hyperon coupling constants are fixed by the corresponding hyperon potentials, $U_H = x_{\omega H} V - x_{\sigma H} S$, where $V = g_{\omega N} \omega_0$ and $S = g_{\sigma N} \phi$ are the ω and σ field strengths at the saturation density [21, 22]. As discussed in Ref. [23], Λ is known to experience an attractive potential, $U_\Lambda = -28$ MeV, in hypernuclear matter. Recently, some authors suggested that Σ^- may feel repulsive potential at high densities [24–26], which was supported by the absence of bound states in a recent Σ hypernuclear search [27]. Therefore, the repulsive potential of Σ , $U_\Sigma = 30$ MeV, is adopted in our calculations as in [28]. The attractive potential of Ξ , $U_\Xi = -18$ MeV, is adopted from Ξ -N interaction [15]. The obtained σ meson-hyperon coupling constants are listed in Table 1. As mentioned before, the vector and isovector meson-hyperon couplings are fixed by $SU(6)$ quark symmetry [29]:

$$g_{\omega\Lambda} = g_{\omega\Sigma} = 2g_{\omega\Xi} = \frac{2}{3}g_{\omega N}, \quad (27)$$

$$g_{\rho\Lambda} = 0, \quad (28)$$

$$g_{\rho\Sigma} = 2g_{\rho\Xi} = 2g_{\rho N}, \quad (29)$$

$$g_{\delta\Lambda} = 0, \quad (30)$$

$$g_{\delta\Sigma} = 2g_{\delta\Xi} = 2g_{\delta N}. \quad (31)$$

Table 1. The σ meson-hyperon coupling constants obtained from hyperon potentials in the VF-RMF and NL-RMF models.

parameters	VF-RMF model		NL-RMF model	
	VF ρ	VF $\rho\delta$	NL ρ	NL $\rho\delta$
$x_{\sigma\Lambda}$	0.62	0.64	0.61	0.62
$x_{\sigma\Sigma}$	0.37	0.38	0.36	0.37
$x_{\sigma\Xi}$	0.33	0.34	0.32	0.33

The in-medium masses of baryons and mesons can be obtained by calculating the loop corrections to their self-energies, see Fig. 1. As discussed before, because the meson propagators appearing in the baryon self-energies are calculated at zero four-momentum transfer (see Fig. 1(a)), we have to use the off-shell in-medium meson masses in the tadpole loop calculations for self

consistency. The off-shell in-medium meson masses in the hyperonic neutron star matter are shown in Fig. 2. It is found that the off-shell in-medium meson masses increase with the increase of the total baryon density (the sum of the densities of $n, p, \Lambda, \Sigma^-, \Sigma^0, \Sigma^+, \Xi^-, \Xi^0$). The introduction of the density dependence of in-medium meson masses is the critical effect of VF corrections.

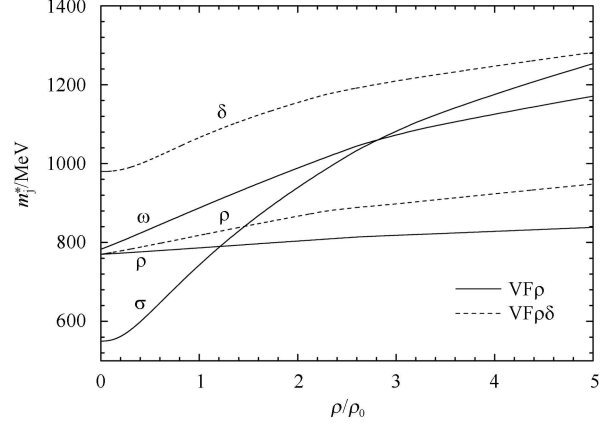


Fig. 2. Off-shell in-medium meson masses (m_j^*) in the hyperonic neutron star matter as a function of the total baryon density with the meson-hyperon couplings fixed by hyperon potentials and $SU(6)$ quark symmetry in the VF-RMF model.

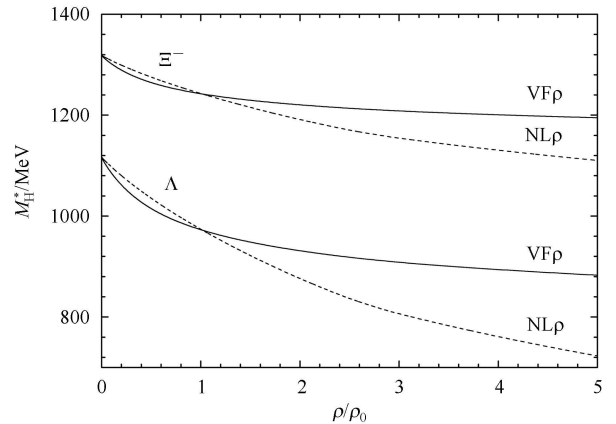


Fig. 3. The in-medium masses of hyperons, M_H^* ($H = \Lambda, \Xi^-$), as a function of the total baryon density with the meson-hyperon couplings fixed by hyperon potentials and $SU(6)$ quark symmetry in different models.

In this work, hyperons are included in the VF-RMF model. The in-medium masses of hyperons play an important role in the calculations of EoS. Fig. 3 shows the in-medium masses of Λ and Ξ^- as a function of the total baryon density in different models for a comparison. It is found that the VF corrections soften the decrease of the in-medium hyperon masses at high densities. This

implies the softer EoS for the hyperonic neutron star matter obtained in the VF-RMF model than that in the NL-RMF model.

Now we define the relative population of the baryon B as the ratio of the density of B and the total baryon density. Fig. 4 and Fig. 5 show the relative populations as a function of the total baryon density with the meson-hyperon couplings fixed by hyperon potentials and $SU(6)$ quark symmetry in the NL-RMF model and the VF-RMF model, respectively. Comparing these two figures, we find that the VF corrections lead to later emergence of all hyperons. Meanwhile, the VF corrections reduce the population of Ξ^0 while they enlarge the population of leptons. We can see that $\Sigma^{(\pm,0)}$ experience such a strong repulsion that they do not appear at all in the density range found in the neutron stars. This is consistent with the fact that Σ^- is hardly stabilized in the hypernuclear matter [28]. In the VF-RMF model, the δ field effects shift the thresholds of all the hyperons to lower densities. On the other hand, the δ field effects shift the thresholds of Λ and Ξ^- to lower densities while shifting the threshold of Ξ^0 to higher density in the NL-RMF model. The δ field effects on the population of baryons and leptons are not apparent in both models.

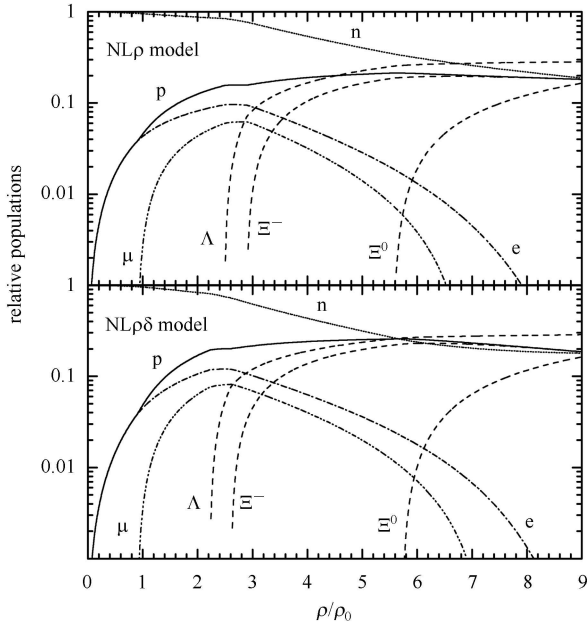


Fig. 4. The relative populations as a function of the total baryon density with the meson-hyperon couplings fixed by hyperon potentials and $SU(6)$ quark symmetry in the NL-RMF model.

Figure 6 shows the EoS, pressure vs. the total baryon density, for the hyperonic neutron star matter with the meson-hyperon couplings fixed by hyperon potentials

and $SU(6)$ quark symmetry in different models. The insert of Fig. 6 presents the EoS for the nucleonic ($npe\mu$) neutron star matter for a comparison. We can see that the introduction of hyperons and VF corrections soften the EoS greatly. Unlike the case of the nucleonic neutron star matter, the presence of the δ field stiffens the EoS at first, and then from the appearance of Λ and Ξ^- till higher densities softens the EoS for the hyperonic neutron star matter. This is because the attractive

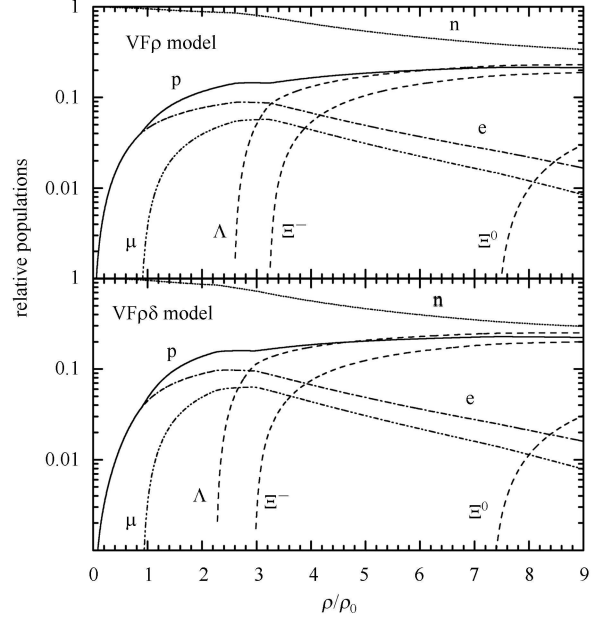


Fig. 5. The relative populations as a function of the total baryon density with the meson-hyperon couplings fixed by hyperon potentials and $SU(6)$ quark symmetry in the VF-RMF model.

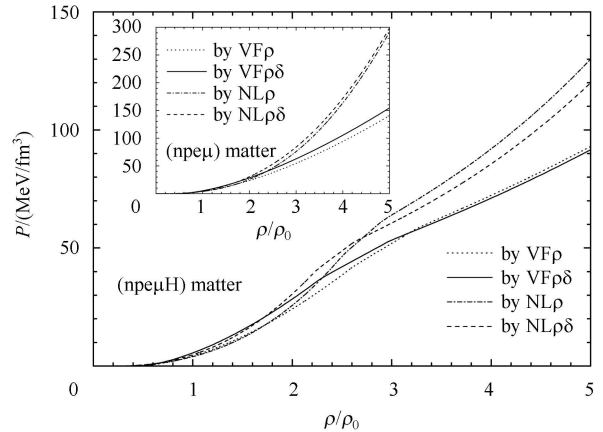


Fig. 6. The EoS for the hyperonic neutron star matter with the meson-hyperon couplings fixed by hyperon potentials and $SU(6)$ quark symmetry. The insert is the EoS for the nucleonic neutron star matter.

Table 2. The maximum masses (M_S in units of M_\odot), the corresponding radii and the central densities of hyperonic neutron stars and nucleonic neutron stars. The meson-hyperon couplings are fixed by hyperon potentials and $SU(6)$ quark symmetry.

neutron star	properties	VF-RMF model		NL-RMF model	
		VF ρ	VF $\rho\delta$	NL ρ	NL $\rho\delta$
hyperonic neutron star npe μ H	M_S/M_\odot	1.33	1.43	1.57	1.59
	R/km	12.37	13.13	12.02	13.036
	ρ_c/ρ_0	4.91	4.89	5.76	4.63
nucleonic neutron star npe μ	M_S/M_\odot	1.52	1.66	2.09	2.12
	R/km	10.85	11.82	10.93	11.37
	ρ_c/ρ_0	7.58	6.36	6.66	6.29

effects of Λ and Ξ^- are larger than the repulsive effects of the δ field. Such effects of the δ field reflect the complicated nature of interactions between mesons and hyperons in the hyperonic neutron star matter, which needs in depth study in the future.

The properties of neutron stars can be calculated by solving TOV equations. Fig. 7 shows the correlation between the neutron star masses and the corresponding radii for hyperonic and nucleonic neutron stars with meson-hyperon couplings obtained by hyperon potentials and $SU(6)$ quark symmetry in different models. The obtained maximum masses, the corresponding radii and the central densities are presented in Table 2. As pointed out in Ref. [30], the introduction of hyperons leads to the reduction of the maximum neutron star masses due to the Pauli principle effects. We can see from Table 2 that our results are consistent with this statement. Furthermore, we can see that the VF corrections also result in the reduction of the maximum masses of neutron stars. The presence of the δ field enlarges the maximum masses and radii of neutron stars.

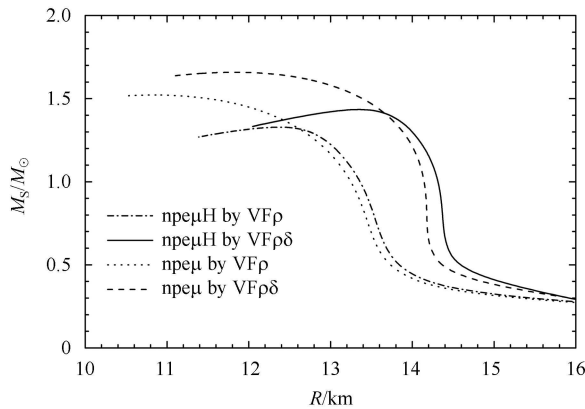


Fig. 7. The masses of neutron stars as a function of the radii of neutron stars in the VF-RMF model. The meson-hyperon couplings are fixed by hyperon potentials and $SU(6)$ quark symmetry.

In the literature, there are various approaches to determine the meson-hyperon couplings [9, 29, 31]. In order to see the dependence of our results on the meson-

hyperon couplings, we also compare our results by adopting the meson-hyperon couplings derived from the quark counting method, $x_{jH} = \sqrt{2/3}$ [31], and the universal meson-hyperon couplings, $x_{jH} = 1$ [9].

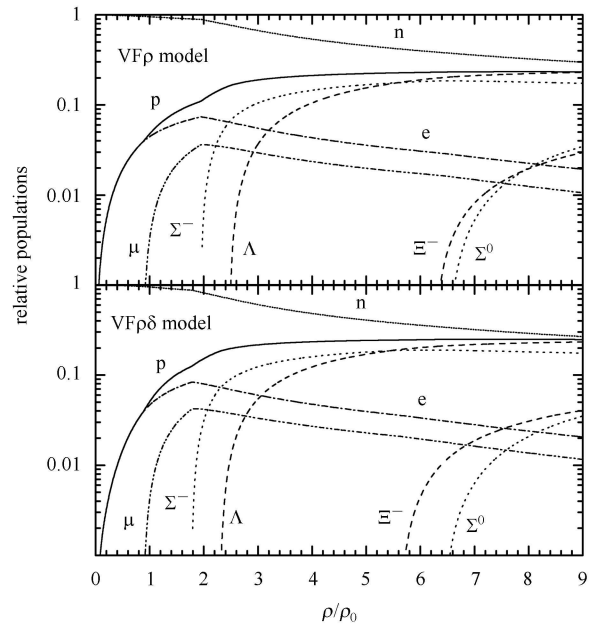


Fig. 8. The relative populations as a function of the total baryon density with quark counting meson-hyperon couplings in the VF-RMF model.

Figure 8 and Fig. 9 show the relative populations as a function of the total baryon density with the quark counting and universal meson-hyperon coupling choices, respectively. We can see that Σ^- is the first hyperon to appear due to its low mass and favored charge [32]. For both kinds of meson-hyperon couplings, the presence of δ field leads to earlier emergence of hyperons. For both the quark counting and the universal meson-hyperon coupling choices, the populations of nucleons dominate in the whole density region. However, as can be seen from Fig. 5, the population of Λ exceeds that of the proton at high densities when we adopt the meson-hyperon couplings fixed by hyperon potentials and $SU(6)$

quark symmetry. Comparing Fig. 8 and Fig. 9 with Fig. 5, we can see that the onset of Ξ^- is greatly reduced in Fig. 5 to compensate the absence of Σ^- in order to keep charge neutrality [9]. We note that Ξ^0 and Σ^+ will appear beyond the maximum density considered here, $9\rho_0$, when we adopt the quark counting and universal meson-hyperon coupling choices.

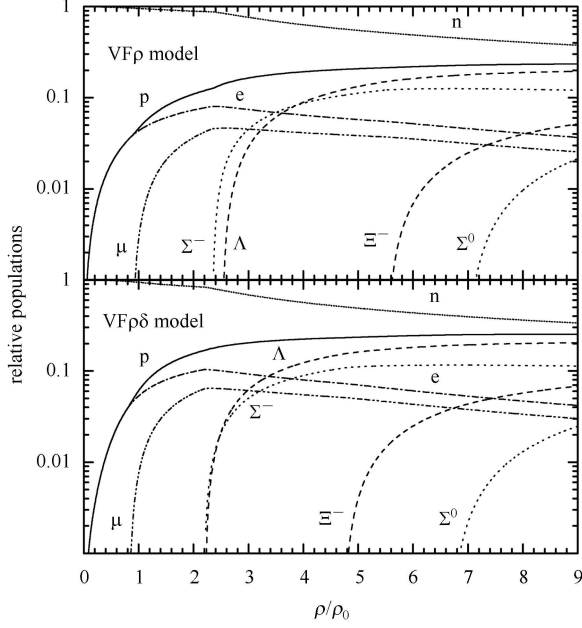


Fig. 9. The relative populations as a function of the total baryon density with the universal meson-hyperon coupling choice in the VF-RMF model.

Figure 10 shows the masses of hyperonic neutron stars as a function of the neutron star radii with the quark counting and universal meson-hyperon couplings in the VF-RMF model. Comparing Fig. 10 with Fig. 7, it is obvious that the properties of hyperonic neutron stars are sensitive to the meson-hyperon couplings. We can see that the weaker the meson-hyperon couplings the lower the masses and radii of hyperonic neutron stars obtained. As in Fig. 7, the presence of the δ field also increases the masses and radii of hyperonic neutron stars.

Table 3 displays the properties of hyperonic neutron stars with the quark counting and universal meson-hyperon couplings in the VF-RMF model. Comparing Table 3 with Table 2, we can see that the influence of meson-hyperon couplings on our results are distinct. With the adoption of the universal meson-hyperon couplings, the obtained maximum hyperonic neutron star masses are higher than those obtained by adopting the other two kinds of meson-hyperon couplings and even higher than the maximum masses obtained in the case of nucleonic neutron stars. As discussed in Refs. [21, 30], the conversion of nucleons to hyperons are energetically favored. The inclusion of hyperons softens the EoS and

consequently reduces the maximum masses of neutron stars because the Pauli principle minimizes the total energy at a given density. Based on the above discussion, the choice of universal hyperon couplings is not appropriate for our model. It is found that the weaker the meson-hyperon couplings the lower maximum masses and the corresponding radii of hyperonic neutron stars are obtained. The adoption of meson-hyperon couplings fixed by hyperon potentials and $SU(6)$ quark symmetry results in the softest EoS of the hyperonic neutron matter and hence leads to the lowest maximum masses of hyperonic neutron stars. We also find that the maximum masses and radii of hyperonic neutron stars increase when the δ field presents in the VF-RMF model.

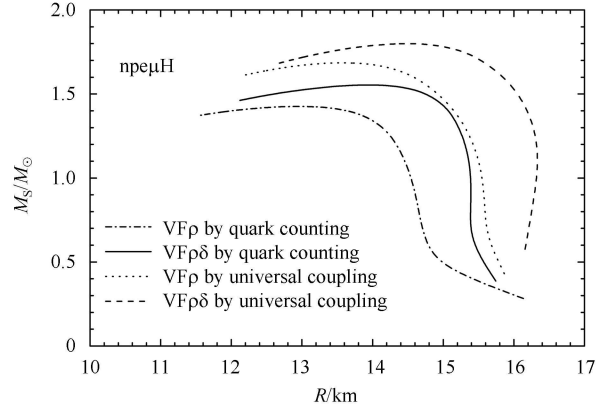


Fig. 10. The masses of hyperonic neutron stars as a function of the radii of hyperonic neutron stars with the quark counting and universal meson-hyperon couplings in the VF-RMF model.

Table 3. The maximum mass (M_S in units of M_\odot), the corresponding radii and the central densities of hyperonic neutron stars with the quark counting and universal meson-hyperon coupling choices in the VF-RMF model.

meson-hyperon couplings	properties	VF-RMF model	
		VF ρ	VF $\rho\delta$
$x_{jH} = \sqrt{2/3}$	M_S/M_\odot	1.43	1.55
	R/km	12.98	13.98
	ρ_c/ρ_0	4.71	3.98
$x_{jH} = 1$	M_S/M_\odot	1.69	1.80
	R/km	13.59	14.50
	ρ_c/ρ_0	4.48	3.89

4 Summary

In this work, we investigate the properties of the hyperonic neutron star matter in the extended VF-RMF model. The interactive hyperons and free leptons are introduced into the relativistic Lagrangian density. The VF effects are included by taking into account the loop

corrections in the hadron self-energies. In our calculations, we replace all the meson masses by the off-shell in-medium meson masses since the propagators of mesons in the tadpole diagrams of baryon self-energies carry zero-momenta. With the VF corrections the in-medium baryon and meson masses are dependent on the total baryon density.

In general, the interactions between different mesons and hyperons should be different. We prefer to adopt the σ meson-hyperon couplings derived from the hyperon potentials with the vector and isovector meson-hyperon couplings fixed by the $SU(6)$ quark symmetry. We find that the off-shell in-medium meson masses increase with the increase of total baryon density. The in-medium masses of hyperons decrease slower at high densities when the VF corrections are introduced. The density dependence of off-shell in-medium meson masses and in-medium hyperon masses influences the behavior of the EoS for the hyperonic neutron star matter directly. The introduction of hyperons softens the EoS since the Pauli principle minimizes the total energy at a given density. The results obtained in the VF-RMF model are compared with those obtained in the NL-RMF model. It is found that the VF corrections soften the EoS for the hyperonic neutron star matter and hence the maximum masses of hyperonic neutron stars are reduced. $\Sigma^{(\pm,0)}$ are absent in the range of densities found in neutron stars because they feel a strong repulsion in this meson-hyperon couplings choice.

Then, the dependence of our results on the meson-hyperon couplings is studied. We use another two choices for meson-hyperon couplings for a comparison: one is derived from the quark counting method, the other is the so-called universal couplings. It is found that the properties of hyperonic neutron stars are sensitive to the meson-hyperon couplings. The weaker the meson-hyperon couplings the lower the maximum masses of hyperonic neutron stars are obtained. For the quark counting and universal coupling choices, $\Sigma^{(\pm,0)}$ are present and the populations of nucleons dominant in the whole region of total baryon densities. The maximum masses of hyperonic neutron stars obtained with the universal meson-hyperon couplings exceed the maximum masses of nucleonic neutron stars. Because the Pauli principle assures that the appearance of hyperons will lower the Fermi energy of baryons and hence will lower the total energy at a given baryon density, the universal meson-hyperon couplings is not appropriate for our model. Taking into account the uncertainty of meson-hyperon couplings, the obtained maximum hyperonic neutron star masses are in the range of $1.33M_{\odot}$ – $1.55M_{\odot}$ (M_{\odot} denotes the mass of the sun) in the VF-RMF model.

The effects of the δ field on hyperonic neutron stars are investigated in the VF-RMF model. Unlike the case

of the nucleonic neutron star matter, we find that the presence of the δ field stiffens the EoS at first and then softens the EoS from the appearance of Λ and Ξ^- till higher densities for the hyperonic neutron star matter. Such effects of the δ field on the EoS reflect the complicated interactions in the hyperonic neutron star matter. In addition, the presence of the δ field enlarges the maximum masses and radii of hyperonic neutron stars. The effects of the δ field on neutron stars are more apparent when the VF corrections are included.

As discussed in Ref. [2], the exchange diagram contributions only provide small corrections to the EoS for nuclear matter in the RMF approach at high densities. We simply extend this statement to the case of the hyperonic neutron star matter as the first step to study the VF effects by including hyperons in our model. Consequently, we only consider the contributions from tadpole diagrams to the baryon self-energies in the present work.

Quantum Hadrodynamics (QHD) was proposed as a renormalizable theory. Calculations at one-loop level, especially the relativistic Hartree approximation, have been widely used and yielded reasonable descriptions of nuclear ground state properties with a few phenomenological parameters [1, 2, 33–38]. However, two-loop corrections were explicitly calculated with bare vertices and found to be large [39]. This indicated that the loop expansion may not be convergent. Afterwards some authors argued that the internal substructure of hadrons should be taken into account since the loop momentum higher than 5 GeV gives sizable contributions to the energy density (the nucleon radius corresponds to 0.4 GeV in momentum space) [40–42]. They found that the two-loop results with on-shell vertex form factors were significantly smaller than those computed with bare vertices. However, calculations with off-shell vertices have never been carried out and whether one can solve the convergence problem of the loop expansion with the introduction of such form factors is still open to investigation [43, 44].

In recent years, QHD has been evolved into a low energy effective theory which includes πN coupling through the consideration of chiral symmetry and chiral symmetry breaking [45–48]. The loop expansion is applied with the technique of Infrared Regularization, which has the advantage to separate the self energy contribution into soft and hard parts. The hard part can be absorbed into counterterms already present in the effective Lagrangian, and can be removed either by field redefinitions or by fitting the empirical data. The soft part is nonlocal and must be calculated explicitly. Calculations at one- to three-loop levels were carried out to verify that the coupling parameters remain natural when fitted to the empirical properties of equilibrium nuclear matter [45–48]. It is found that while two-loop and three-loop

contributions are not large, they are not negligible either. The energy contributions decrease order by order in loops when a reasonable cutoff is chosen. However, whether the loop expansion of the effective theory is indeed practical is still uncertain [46–48].

Calculations at one-loop level are phenomenologically

successful and may be a viable starting point for the description of high density nuclear matter at present. It will be very interesting to study the VF effects at one-loop level on the properties of hyperon-hyperon interaction, kaon condensation and unconfined quarks in the core of neutron stars in the future.

References

- 1 Walecka J D. *Ann. Phys.*, 1974, **83**: 491
- 2 Serot B D, Walecka J D. *Adv. Nucl. Phys.*, 1986, **16**: 1
- 3 Sugahara Y, Toki H. *Nucl. Phys. A*, 1994, **579**: 557
- 4 Müeller H, Serot B D. *Phys. Rev. C*, 1995, **52**: 2072
- 5 Müeller H, Serot B D. *Nucl. Phys. A*, 1996, **606**: 508
- 6 LIU B, Greco V, Baran V et al. *Phys. Rev. C*, 2002, **65**: 045201
- 7 LIU B, GUO H, Di-Toro M et al. *Eur. Phys. J. A*, 2005, **25**: 293
- 8 Glendenning N K. *Phys. Lett. B*, 1982, **114**: 392
- 9 Glendenning N K. *Astrophys. J.*, 1985, **293**: 470
- 10 SHEN H. *Phys. Rev. C*, 2002, **65**: 035802
- 11 Espíndola A L, Menezes D P. *Phys. Rev. C*, 2002, **65**: 045803
- 12 Menezes D P, Providência C. *Phys. Rev. C*, 2004, **70**: 058801
- 13 Gaitanos T, Di-Toro M, Typel S et al. *Nucl. Phys. A*, 2004, **732**: 24
- 14 Baran V, Colonna M, Greco V et al. *Phys. Rep.*, 2005, **410**: 335
- 15 Schaffner-Bielich J, Gal A. *Phys. Rev. C*, 2000, **62**: 034311
- 16 MI A J, ZUO W, LI A. *Int. J. Mod. Phys. E*, 2008, **17**: 1293
- 17 Bhattacharyya A, Ghosh S K, Phatak S C. *Phys. Rev. C*, 1999, **60**: 044903
- 18 GUO X H, LIU B, WENG M H. *Phys. Rev. C*, 2009, **79**: 054316
- 19 Kurasawa H, Suzuki T. *Nucl. Phys. A*, 1988, **490**: 571
- 20 Tolman R C. *Phys. Rev.*, 1939, **55**: 364; Oppenheimer J R, Volkoff G M. *Phys. Rev.*, 1939, **55**: 374
- 21 Glendenning N K, Moszkowski S A. *Phys. Rev. Lett.*, 1991, **67**: 2414
- 22 Mareš J, Dover C B, Gal A et al. *Phys. Rev. Lett.*, 1993, **71**: 1328
- 23 Millener D J, Dover C B, Gal A. *Phys. Rev. C*, 1988, **38**: 2700
- 24 Batty C J, Friedman E, Gal A. *Phys. Lett. B*, 1994, **355**: 273
- 25 Mareš J, Friedman E, Gal A et al. *Nucl. Phys. A*, 1995, **594**: 311
- 26 Friedman E, Gal A. *Phys. Rep.*, 2007, **452**: 89
- 27 Bart S, Chrien R E, Franklin W A et al. *Phys. Rev. Lett.*, 1999, **83**: 5238
- 28 SHAO G Y, LIU Y X. *Phys. Rev. C*, 2009, **79**: 025804
- 29 Schaffner J, Mishustin I N. *Phys. Rev. C*, 1996, **53**: 1416
- 30 Glendenning N K. *Phys. Rev. C*, 2001, **64**: 025801
- 31 Moszkowski S A. *Phys. Rev. D*, 1974, **9**: 1613
- 32 Rios A, Polls A, Ramos A et al. *Lect. Notes Phys.*, 2004, **652**: 217
- 33 Perry R J. *Phys. Lett. B*, 1986, **182**: 269; *Nucl. Phys. A*, 1987, **467**: 717
- 34 Fox W R. *Nucl. Phys. A*, 1989, **495**: 463
- 35 Furnstahl R J, Price C E. *Phys. Rev. C*, 1990, **40**: 1398; Furnstahl R J, Price C E. *Phys. Rev. C*, 1990, **41**: 1792
- 36 Von-Eiff D, Pearson J M, Stocker W et al. *Phys. Rev. C*, 1994, **50**: 831
- 37 Faessler A, Buchmann A J, Krivoruchenko M I. *Phys. Rev. C*, 1998, **57**: 1458
- 38 Haga A, Tamenaga S, Toki H et al. *Phys. Rev. C*, 2004, **70**: 064322
- 39 Furnstahl R J, Perry R J, Serot B D. *Phys. Rev. C*, 1989, **40**: 321
- 40 Prakash M, Ellis P J, Kapusta J I. *Phys. Rev. C*, 1992, **45**: 2518
- 41 Friedrich R, Wehrberger K, Beck F. *Phys. Rev. C*, 1992, **46**: 188
- 42 Serot B D, TANG H B. *Phys. Rev. C*, 1995, **51**: 969
- 43 Serot B D, Walecka J D. *Int. J. Mod. Phys. E*, 1997, **6**: 515
- 44 Furnstahl R J, Serot B D. *Comments Nucl. Part. Phys.*, 2000, **2**: A23
- 45 Furnstahl R J, Serot B D, TANG H B. *Nucl. Phys. A*, 1997, **615**: 441
- 46 McIntire J, HU Y, Serot B D. *Nucl. Phys. A*, 2007, **794**: 166
- 47 HU Y, McIntire J, Serot B D. *Nucl. Phys. A*, 2007, **794**: 187
- 48 McIntire J. *Ann. Phys.*, 2008, **323**: 1460